Venezia 2021

Programma di ricerca scientifica per una laguna "regolata"

Linea 2.2

Inquinanti prioritari e rilascio di sostanze pericolose dal sedimento

D2.2.4.2

Rapporto sui risultati della prima sperimentazione

J.-L. Loizeau, A. Gallorini (University of Geneva)

D. Cassin, J. Dominik, G. Manfè, R. Zonta (CNR-ISMAR)

C. Cosio (University of Reims)

A. Garcia Bravo (Instituto de Ciencias del Mar de Barcelona)

30/11/2020

Summary

1. INTRODUCTION

A main goal of the research of Line 2.2 is to improve the understanding of hydrodynamic and biogeochemical factors that favour the production and export from Venice Lagoon sediments of methylmercury (MMHg), particularly under the changing physico-chemical and biological conditions linked to the implementation of the MOSE system, but also to rising water temperatures as a result of climate change.

The complex analyses on water and sediment samples obtained from the first experiment (November 2019) of the investigation on MMHg have undergone significant slowdowns, due to the health emergency from Covid-19, starting in March 2020. The closure of the analysis laboratories and the subsequent access restrictions have in fact complicated the performance of the analytical activities.

After the relaxation, in the summer, of the restrictions due to the health emergency - despite a complicated logistical situation - an attempt was made to make up for the accumulated delays and a new planning of activities was formulated.

The second field experiment, scheduled for the period May - June 2020, was forced to postpone for a whole year; in fact, this activity must be carried out in late spring, to compare the results with those obtained in the first autumn experiment of 2019.

This Report, not provided for by the project specification, is drawn up to describe the progress of the activities given the delays that have occurred and the changes that have been introduced in the planning of activities, due to the health emergency.

2. SAMPLING AND ANALYTICAL METHODS

2.1 November 2019 sampling campaign

The experiment is based on the collection and incubation of sediment cores. A first field campaign to collect sediment cores took place from November 18th to 23rd in the Venice Lagoon. Two sampling locations were selected based on previous investigations on sediment characteristics (Zonta et al., 2019): Osellino (OS) and San Giuliano (SG) (Fig. 1). A total of 7 sediment cores on each site were collected on November 20th: Plexiglas tubes (14 cm diameter) were driven into the sediment manually by a diver and the core was collected with the overlying water.

Figure 1. Map of sampling sites location: OS (45°28'28.88"N, 12°17'9.56"E) and SG (45°27'49.30"N, 12°17'42.00"E).

2.2 Core processing

Three cores from each sampling site were directly processed under controlled atmosphere (in glove box filled with nitrogen), to avoid the oxidation of reduced sediments and pore water. These cores are named OS6, OS7 and OS8 for the Osellino site, and SG6, SG7 and SG8 for the San Giuliano site. Prior to sediment sub-sampling, overlying water was collected with a peristaltic pump and filtered. In the glovebox (Fig. 2), the sediments were vertically extruded and two sediment layers sub-sampled, corresponding to 0-2 and 2-4 cm depth. These cores correspond to the initial situation ("fresh cores"), that is cores not incubated.
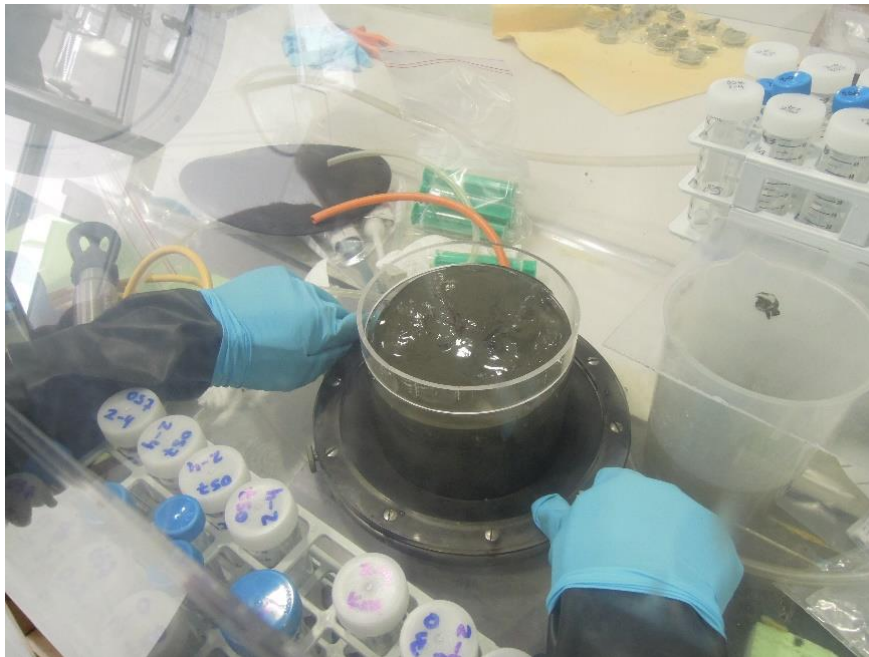
Figure 2. Sediment core subsampling in controlled atmosphere.

For each site, three cores were sealed and stored in a dark room at constant temperature (14°C) to simulate a stagnation of the water column. After approximately 2 days of incubation, these cores were processed following the same procedure as the fresh cores. These cores correspond to the "final" situation, that is after incubation ("incubated cores").

Incubation times were OS9 (44.4 h), OS10 (45.6 h) and OS11 (44.4 h) for the Osellino site, and SG6 (47.0 h), SG7 (49.0 h) and SG8 (50.3h) for the San Giuliano site.

The different samples collected from each core and the analyses performed are presented in Table 1.

Table 1. Sample type and analyses preformed on sediment cores.

Sample type	Grain size	Organic matter characterization	Trace elements	THg	MeHg	Km/Kd	DNA
Raw overlying water				X	X		
Filtered overlying water		X	X	X	X		
Filtered pore water				X	X		
Sediment	X	X	X	X	X	X	X

The overlying water was filtered with Sterivex filters (0.45 µm). Pore water of the two sediment layers (0-2 and 2-4 cm depth) was extracted by sediment centrifugation (4000 rpm, 60 min, 4°C) and subsequent filtration (Sterivex 0.45 µm) in controlled atmosphere (glovebox). Aliquots of fresh sediment were directly used for sediment grain size determination and conserved frozen at -20°C in life-guard for DNA extraction. The remaining sediments were freeze-dried for further analyses. Water samples were kept at 4°C prior to analyses.

The total number of collected samples correspond to 24 overlying water (12 raw and 12 filtered), 24 filtered pore water, 24 sediments, 96 Hg isotope-spiked sediments, and 48 lifeguard-fixed sediments (DNA extraction).

2.3 Methods of analyses

2.3.1. Water content and Loss On Ignition

Sediment water content was measured directly at CNR-ISMAR lab by weight difference after drying in an oven (60°C). Bulk organic matter content was estimated by loss on ignition (LOI), determined by weight difference after burning dry sediment 1h at 550°C (Heiri et al., 2001). Uncertainties in water content and LOI determinations is between 0.5 and 0.7%.

2.3.2. Grain size distribution

Sediment grain size distribution was determined by laser diffraction using a Laser-Coulter LS-100 diffractometer (Beckman-Coulter, USA). Fresh sediment sample were measured after 10-min sonication, following the procedure described by Loizeau et al. (1994).

2.3.3. Total organic carbon, mineral carbon, Hydrogen Index (HI) and Oxygen Index (OI)

Characterization and quantification of the organic matter were performed on powdered bulk sediment at the Institute of Earth Sciences at the University of Lausanne using Rock-Eval 6, (Behar et al., 2001; Espitalié et al., 1985a, 1985b). The determined parameters were total organic carbon (TOC), the Hydrogen Index (HI as mg HC g^{-1} TOC) and the Oxygen Index (OI as mg CO_2 g^{-1} TOC). The standard used was IFP 160000 Rock-Eval, and the analyses were carried out on 50-100 mg of powdered dry sediment under standard conditions. Analytical precision was better than 0.05 wt % (1s) for TOC, 10 mg HC g^{-1} TOC (1s) for HI, and 10 mg CO_2 g^{-1} TOC (1s) for OI.

2.3.4. Total carbon and nitrogen

Total nitrogen and carbon concentrations were determined in a CHN Elemental Analyzer (Thermo Finnigan Flash EA 1112) using approximately 10 mg of dry powdered sediment. Precision was better than 1% based on an internal standard, and replicate samples.

2.3.5. Dissolved organic carbon and fluorescence of organic matter

Water samples for the determination of dissolved organic carbon (DOC) concentration were stored in 550°C oven-muffled glass bottles after filtration with Sterivex 0.45 μm and were acidified with 2 M HCl (pro analysis, Merck). DOC measurements were performed with a TOC-5000A analyzer (Shimatzu, Kyoto, Japan).

Coloured and fluorescent dissolved organic matter (CDOM and FDOM) was characterized in samples filtered with Sterivex 0.45μm and in the dark at 4°C after filtration at the Institute of Marine Sciences in Barcelona (CSIC). Absorbance spectra and excitation-emission matrices were obtained simultaneously using a Horiba Aqualog instrument (Aqualog-UV-Vis, Horiba JobinYvon, Japan) against freshly produced Milli-Q grade water. The fluorescence spectrophotometer has a routine protocol before running samples that involves i) instrument validation (ensuring the signal: noise ratio <20,000 counts, ii) ensuring the excitation lamp is calibrated to a given wavelength (maximum intensity at 467 nm), and iii) the emission energy is calibrated using pure water at an emission of 397 nm and an excitation of 350 nm. Fluorescence spectra were collected

across excitation wavelengths (λ_{ex}) 250-445 nm at 5 nm increments and across emission wavelengths (λ_{em}) ranging from 300 to 600 nm. Bandpass and resolution were 5 nm. All spectra were measured in a 1 cm quartz cuvette and automatically blank-subtracted, corrected (inner-filter and scatter corrections) and normalized to Raman Units (R.U.) using R package statRdom (Pucher et al., 2019). Samples were measured for fluorescence at a 2 s integration time.

Peak picking was used to define the relative intensity of four common peaks across the EEM including the Peak A (λ_{ex}: 260 nm, λ_{em}: 400-460 nm), Peak C (λ_{ex}: 320-360 nm, λ_{em}: 420-460 nm), and Peak M (λ_{ex}: 290-310 nm, λ_{em}: 370-410 nm) associated with soil terrestrial DOM, as well as a protein-like peak T (λ_{ex}: 275 nm, λ_{em}: 340-350 nm) that is considered to be of algal/bacterial origin (i.e. autochthonous to the aquatic environment) (Fellman et al., 2010; Huguet et al., 2009). The summed area of total fluorescence (TF) under the EEMs was used to normalize each of the four peaks, which were expressed as a percent of TF (i.e. %Peak A $1/4$ Peak A/TF x 100). We also calculated three common fluorescence indexes: i) the fluorescence index (FI, calculated as the ratio between emission at wavelengths of 470 and 520 nm, at an excitation of 370 nm), an indicator of source being more microbial (1.7–2) or terrestrial (1.2–1.4) (Cory et al., 2007; McKnight et al., 2001), ii) the freshness index (calculated as the ratio of emission at 380 nm, divided by the emission maxima between 420 and 435 nm, at an excitation of 310 nm) which reflects the age of OM, with higher values representing more recently produced OM (Parlanti et al., 2000), and iii) the humification index (HIX, ratio of peak areas across an emission spectra [435-480 nm/300-345 nm]), indicating the degree of humification (Zsolnay et al., 1999). The absorbance at 254 nm (A254) was used to calculate carbon specific absorbance (SUVA254), a commonly used metric of the degree of aromaticity, as A254/DOC concentration normalized to a 1 m path length (L mg C^{-1} m^{-1}) (Weishaar et al., 2003).

2.3.6. Trace elements

Trace elements were determined by inductively coupled plasma mass spectrometry (ICP-MS, model 7700 series, Agilent). Filtered water samples, acidified with 1% suprapure HNO_3, were directly analysed whereas sediments were digested in Teflon bombs heated to 150°C in analytical grade 2 M HNO_3 according to the Swiss Soil Protection Ordinance (FOEN, 1998). Multi-element standard solutions (0.02, 1, 5, 20, 100 and 200 µg L-1) were used for calibration. The total variation coefficients for triplicate sample measurements were better than 10%.

2.3.7. Total and methyl-mercury

Total Hg in freeze-dried sediment was analysed by cold vapor atomic absorption spectro-photometry (CV-AAS) using a direct mercury analyser DMA-80 III (MWS GmbH, Switzerland). All analyses were conducted in triplicate. The detection limit and working range were 0.01 and 0.05–600 ng, respectively. Concentrations obtained for repeated analyses of the certified reference material never exceeded the specified acceptance range given for the SRM2702 reference material (NIST).

Methylmercury in solid matrix was extracted using a HNO_3 leaching/CH_2Cl_2 extraction method (Liu et al. 2012). The recovery of extractions and analyses of the certified reference material (ERM-CC580) were above 85%. Then the solution was analysed by cold vapor atomic fluorescence spectrometry (CV-AFS), see below.

THg in raw and filtered water samples was determined by oxidation, purge and trap, desorption, and CVAFS (Merx Model III, Brooks Rand, USA) following the EPA 1631 method (US-EPA, 2002).

MeHg in raw and filtered water samples was determined by distillation, aqueous ethylation, purge and trap, desorption, and CVAFS (Merx Model III, Brooks Rand, USA), following the EPA 1630 method (US-EPA, 2001).

2.3.8. Methylation/demethylation rates

Sediments were spiked with Hg isotopes (inorganic [199]Hg and methyl [201]Hg, ISC Science, Spain) and were either directly frozen (1 aliquot) or incubated in a dark room for 24h before to be frozen (3 aliquots). Determination of Hg transformation rates were carried out according to Rodriguez-Gonzalez et al. (2013). Briefly, IHg and MeHg were extracted from 200 mg of freeze-dried sediments with HNO_3 (6 N) under focused microwave treatment and analysed by species specific isotope dilution gas chromatography (GC) hyphenated to an inductively coupled plasma mass spectrometer (ICP-MS) at the University of Pau (France). Methodological detection limits for Hg species were 0.03 ng•g^{-1}. The extraction and quantification were validated with a CRM (IAEA-405) and recoveries were 102±7 and 97±4% for MeHg and IHg, respectively. The concentrations of the added and formed Hg species deriving from the enriched isotopes 199 and 201 were calculated by isotopic pattern deconvolution methodology.

2.3.9. DNA extraction and bacterial community composition

DNA was extracted in triplicate from sediments with the Power Soil RNeasy Extraction Total RNA Kit and RNeasy PowerSoil Elution kit (Qiagen) under sterile conditions according to instructions from the manufacturer. DNA quantity and quality were measured spectrophotometrically. DNA was used for Quantitative PCR quantification of microbial genes linked to Hg biogeochemical cycle as described in Bravo et al. (2018), and Christensen et al. (2016). Metagenomic analysis are planned. Samples will be sent for sequencing together with samples of the next campaign to reduce costs.

2.3.10. Statistical analyses

Data were statistically analysed using R software (R Core Team 2020) and the "corrplot" package (Wei and Simko, 2017).

3. RESULTS AND DISCUSSION

All results are available as Excel files and depicted in the following figures (Figs. 3 to 10).

3.1 Water content and grain size

Water content is very similar in both sites, varying between 64% and 70% in surface layer, and between 57% and 66% in the 2-4 cm layer (Fig. 3). As expected, water contents are slightly lower in the deeper layer. Particle size diameters are in the silt range, with mean grain size usually between 8 and 14 μm. Overall, no trend due to incubation is observed on these parameters.
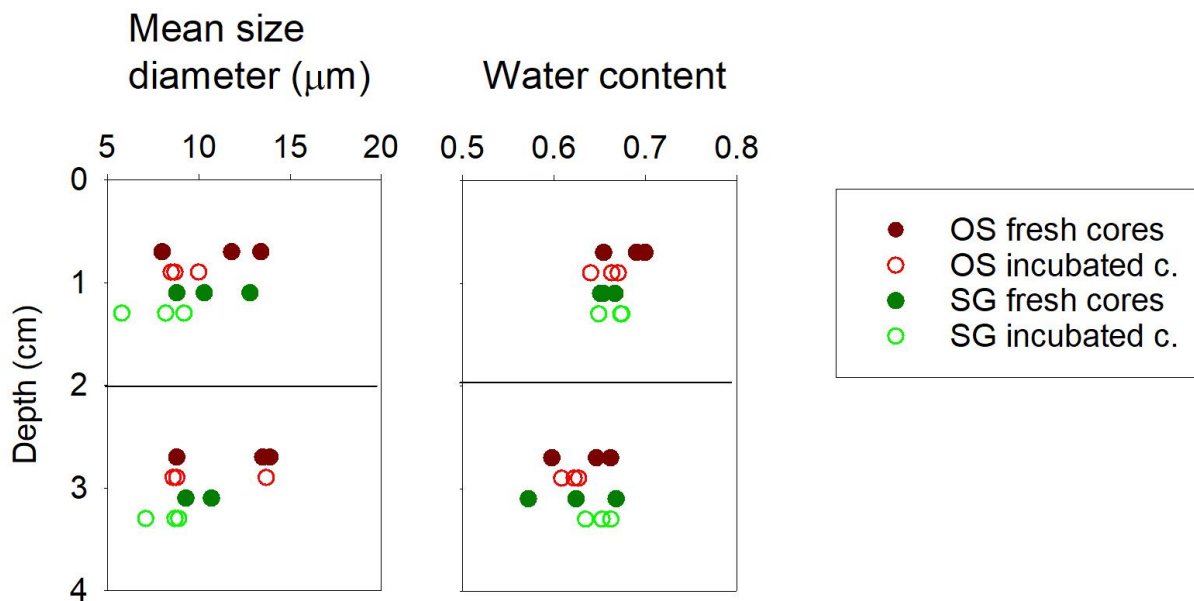
Figure 3. Mean grain size diameter (μm) and water content fraction in the 12 cores. Results are presented for the 0-2 and 2-4 cm depths. Filled circles correspond to initial situation (fresh cores) and open circle correspond to final situation (after ~ 2 days incubation). OS: Osellino site; SG: San Giuliano site (see Fig. 1).

3.2 Particulate organic matter parameters

Several parameters have been measured to characterize the organic matter (OM) present in the sediment (Fig. 4). Loss on ignition (LOI), a surrogate of OM content, varies between 14 and 18%, with a higher variability in the SG site, but no clear difference is observed between the two sites. On the contrary, other parameters (total organic carbon (TOC), N, C/N ratio, Ptot) show higher contents in OS site compared to SG site (Fig. 4). Moreover, there is a clear discrepancy between LOI and TOC results. Their ratio being normally between 2 and 3, it is here between 5 and 10. This may indicate that other components are lost during ignition at 550°C, such as dehydration of clay minerals or metal oxides, loss of volatile salts, or loss of inorganic carbon in minerals (Heiri et al., 2001).

The C/N ratios between 5 and 9 seem to indicate an aquatic origin of the OM, however the HI and OI indexes point to a mixture of fresh and degraded aquagenic, and terrestrial OM.
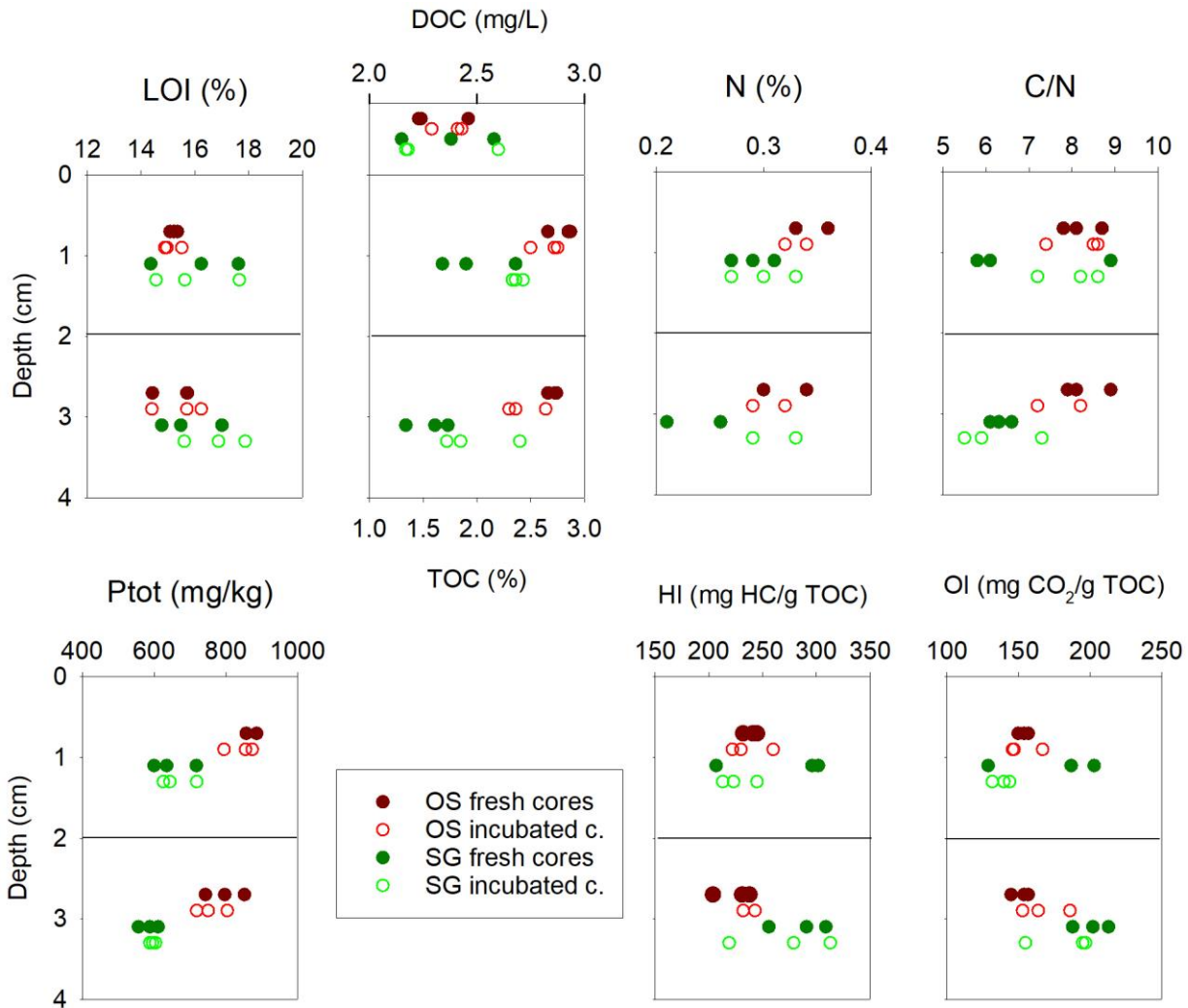
Figure 4. Sediment organic matter parameters. LOI: Loss on ignition, TOC: total organic carbon HI: hydrogen index; OI: oxygen index. DOC: dissolved organic carbon in overlying water is also shown. OS: Osellino site; SG: San Giuliano site.

3.3 Trace elements in sediment

Nine trace elements were analyzed in filtered overlying water and in sediments (Fig. 5). Trace metal concentrations are similar in the different cores collected on the same site and overall lower in the San Giuliano site than in the Osellino site. This is especially noticeable for Co, Cu, Cd, Zn and Pb. As anticipated, no difference is observed before and after core incubations. Dissolved fractions in the overlying water are discussed in section 3.7.

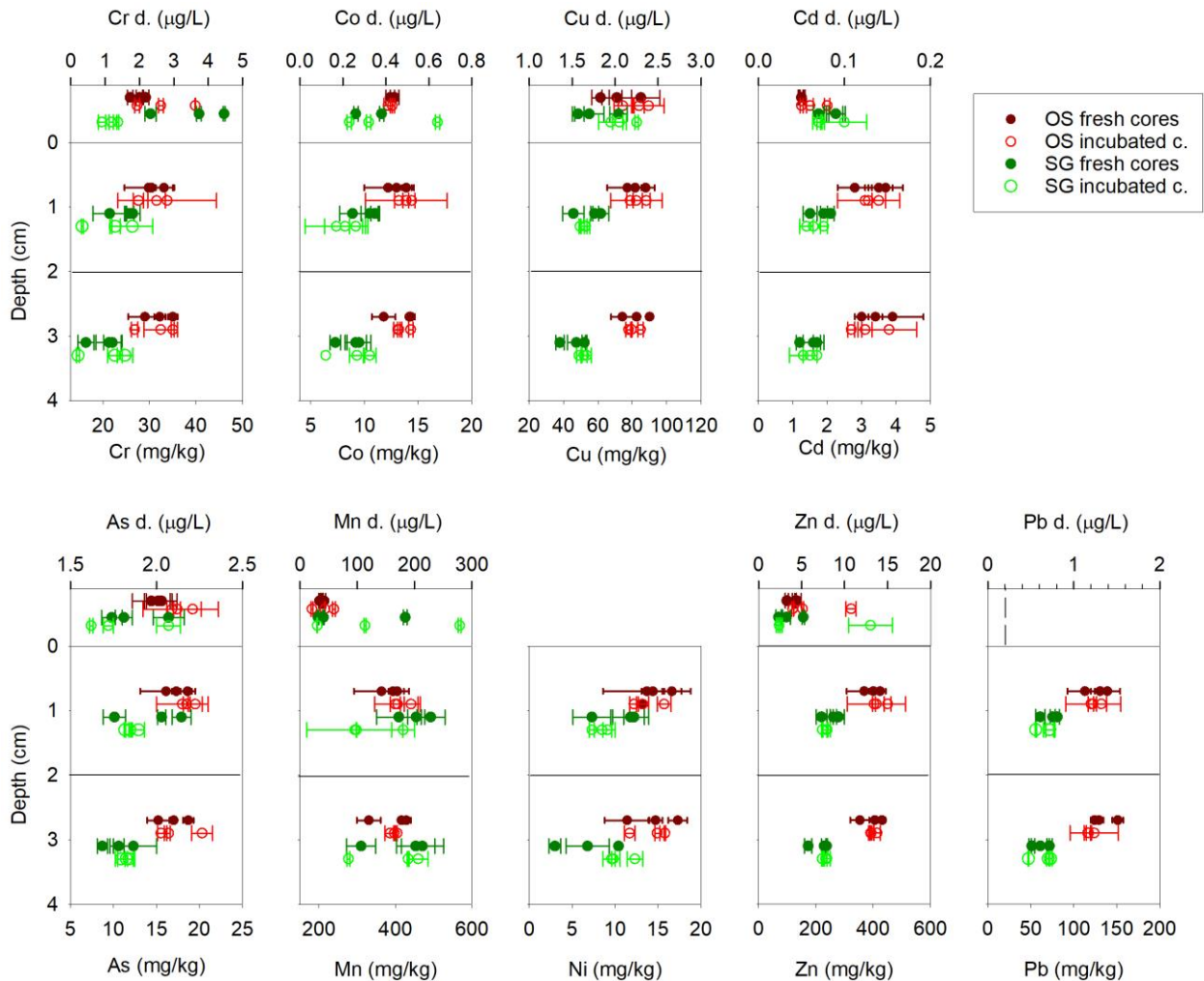Figure 5. Trace elements concentration in filtered overlying waters and sediments before and after incubation. For each metal, the upper graph corresponds to filtered water content, while the remaining part below 0 corresponds to content in sediments (0-2 and 2-4 cm layers). In filtered overlying waters, Ni was not determined because of technical issues, whereas Pb concentrations were below the detection limit (0.2 µg/L, dash line). OS: Osellino site; SG: San Giuliano site.

3.4 Hg in sediments

Total mercury mean and range concentrations in sediments (fresh and incubated cores) are 0.82±0.05 mg/kg (0.72 – 0.89 mg/kg) and 0.95±0.08 mg/kg (0.89 – 1.08 mg/kg) in Osellino and San Giuliano sites, respectively (Fig. 6). No difference was observed between the 0-2 cm and 2-4 cm layers for each site. These results show that the SG site is slightly more contaminated by Hg than the OS site, which is the opposite of what is observed for the other trace elements (see section 3.3).

For methylmercury, the overall concentrations are similar on surface layer, with a larger variability in site SG (Fig. 6). In the deeper layer (2-4 cm), the concentrations are slightly lower on the SG site. However, results have to be examined in more details (Table 2).

In Osellino, considering the uncertainties (1 σ), differences are small if not significant, but a regular pattern is observed. For each core, MeHg concentration is higher in the surface layer than in the underneath layer, except in core OS10. Moreover, mean MeHg concentrations in the surface layers are slightly lower in incubated than in fresh cores (0.048±0.03 vs. 0.56±0.03 µg/kg).

In San Giuliano, differences between the two sediment layers are marked, with always higher MeHg content in the surface than in the underneath layer (as in OS site). Moreover, incubated cores show higher concentrations than fresh cores (0.63±0.14 vs. 0.53±0.11 µg/kg).

MeHg/THg ratios between 0.03 and 0.08 % show that MeHg represents a very low proportion of the total mercury in the sediments. These ratios are similar or slightly lower than those observed by Guédron et al. (2012) at comparable sites and depths in the northeast region of the lagoon.

Table 2. MeHg concentrations (µg/kg) in sediments in fresh and incubated cores.

Sample	MeHg (µg/kg)	1σ - MeHg (µg/kg)	Sample	MeHg (µg/kg)	1σ - MeHg (µg/kg)
Fresh cores					
OS6 0-2	0.59	0.05	SG6 0-2	0.63	0.04
OS6 2-4	0.50	0.05	SG6 2-4	0.31	0.01
OS7 0-2	0.56	0.04	SG7 0-2	0.41	0.03
OS7 2-4	0.52	0.08	SG7 2-4	0.26	0.03
OS8 0-2	0.54	0.04	SG8 0-2	0.55	0.04
OS8 2-4	0.43	0.03	SG8 2-4	0.50	0.06
Incubated cores					
OS9 0-2	0.50	0.03	SG9 0-2	0.72	0.02
OS9 2-4	0.47	0.03	SG9 2-4	0.35	0.02
OS10 0-2	0.49	0.02	SG10 0-2	0.48	0.09
OS10 2-4	0.50	0.03	SG10 2-4	0.28	0.03
OS11 0-2	0.44	0.03	SG11 0-2	0.70	0.01
OS11 2-4	0.41	0.02	SG11 2-4	0.44	0.04

3.5 Hg in overlying and pore waters

Results of mercury in overlying (raw and filtered) water, in sediment and in filtered pore water are presented in Fig. 6. First, it is of note that the detection limits are 0.02 ng/L for THg and between 0.02 and 0.06 ng/L for MeHg. Then most of the MeHg results in overlying water and pore water are close to or below this limit, and therefore not quantifiable.

THg in raw overlying water ranges between 0.87 and 1.43 ng/L in OS site and between 0.45 and 0.65 ng/L in SG site in fresh cores. THg concentration in filtered water in both sites ranges between 0.04 and 0.06 ng/L, that is only slightly higher than the detection limit. The THg concentrations in raw overlying water drop to 0.10 - 0.22 ng/L after incubation (Fig. 6), as the results of suspended particle settling during incubation time.

THg in pore water ranges between 2.0 and 17.1 ng/L in OS site, and between 3.1 and 7.8 ng/L in SG site. No clear difference is observed between depths and sites. Sample OS6 2-4cm shows a high concentration (17.07±1.86 ng/L) compared to other samples.

MeHg concentrations in raw overlying water vary between 0.07 and 0.13 ng/L, whereas concentrations in filtered overlying water show lower range, between 0.03 and 0.07, with the exception of sample SG10 with 0.20 ng/L. This last value is likely biased as the THg concentration in this sample is 0.05 ng/L. No significant differences in MeHg concentrations are observed after incubation.

MeHg concentrations in pore water range from 0.12 to 0.20 ng/L in surface sediment layers, including both sites and fresh and incubated cores, except sample SG6 0-2 cm with 1.76±0.05 ng/L. In the underneath layer, the variability is slightly higher, especially in the SG site (Fig. 6). Again, no clear difference is observed in fresh and incubated cores.

MeHg/THg ratios in pore water vary between 2 and 30 %.
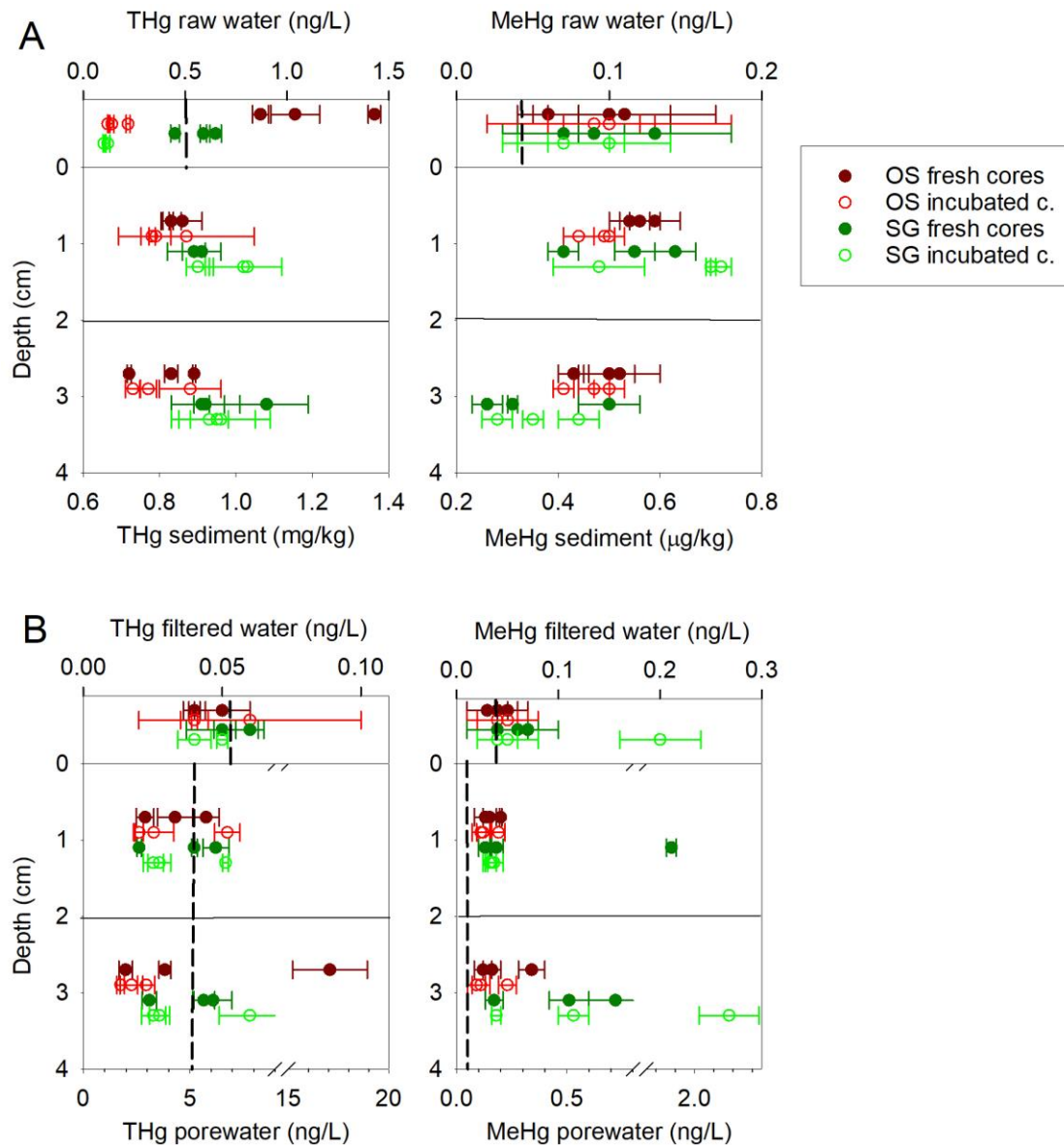
Figure 6. Total mercury (THg) and methylmercury (MeHg) in A) raw overlying water and sediment, and B) filtered overlying water and pore water. Black dash lines indicate the limit of detection. OS: Osellino site; SG: San Giuliano site.

3.6 Microbial functionality of sediments

The abundance of 16s rRNA and dsrA gene for bacteria and sulfate reducing bacteria is similar in both layers and sites (Fig. 7). In OS surface layer, the abundance of the merA gene, required for Hg resistance, is higher than in the underneath layer and SG sediment layers. After incubation merA gene abundance is reduced in OS, suggesting that microbial diversity linked to Hg biogeochemical cycle is modified at OS and not at SG site, where no difference on the merA gene abundance is observed after incubation.

In OS deeper layer hgcA-delta gene, required for Hg methylation by deltaproteobacteria, is higher than in surface layer and SG sediment. Metagenomic analysis will further complete these observations by revealing the global microbial diversity.
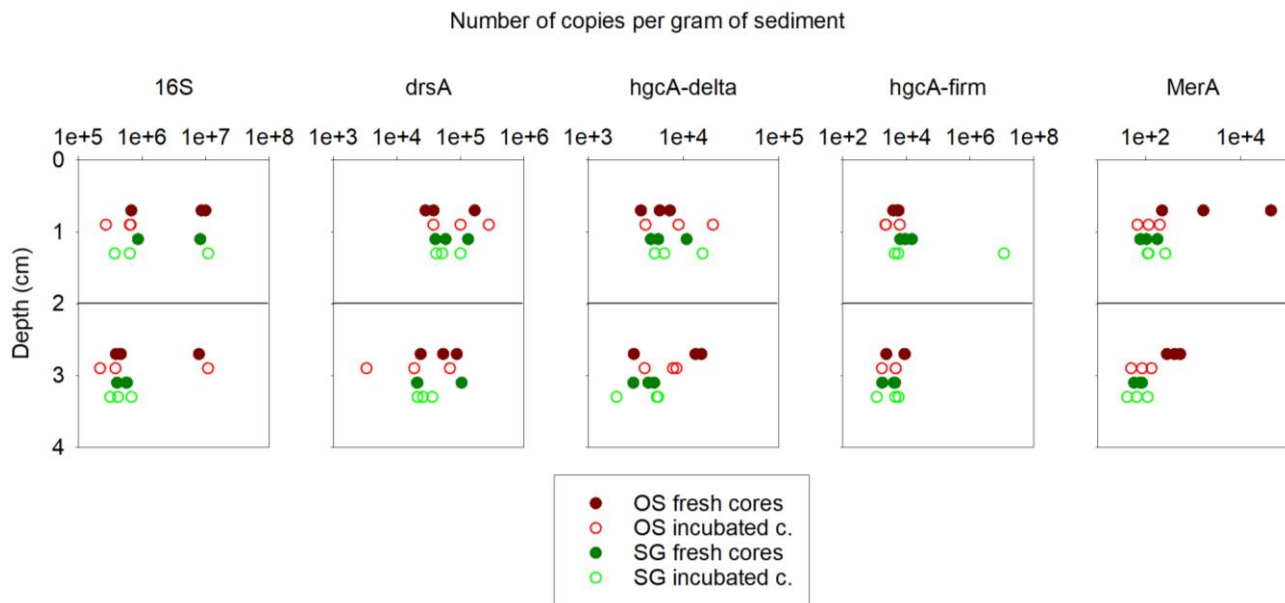

Figure 7. Abundance of selected genes and gene clusters in sediment. OS: Osellino site; SG: San Giuliano site.

3.7 Overlying water

Several parameters have been measured in core overlying water. Dissolved organic carbon (DOC) content varies between 2.1 and 2.6 mg/L, with no difference due to either site or incubation (Fig. 4). Concentration of trace metals in overlying water are similar in both sampling sites, with a slightly higher variability in the SG site. The only observed increase concerns Mn in SG site that reaches almost 300 μg/L in incubated core.

Fluorescence index (FI) can be used to infer DOM sources, with typical values of 1.3–1.4 for terrestrial DOM and of 1.7–2.0 for microbial-derived DOM (McKnight et al., 2001). This index had a mean value of 1.40±0.01 across all samples, indicating that terrestrially derived substances dominate the DOM composition.

Humification index (HIX) had a mean value of 0.85±0.01, similar to those found by Chen et al. (2011) for humic acid isolates (0.83±0.02), pointing the strong influence of terrestrial substances in the overall DOM composition of the studied sites.

Examination of DOC-normalized fluorescence of typical peaks (Coble, 1996) revealed significant differences between sampling sites (Fig. 8). General humics (Peak A) and terrestrial humics (Peak C) were significantly higher at OS compared to SG. Peak M was marginally higher at OS.

No significant differences were found for proteinaceous substances (Peak T) between sites. Differences in the absorbance slope ratio (SR) indicate a lower molecular weight composition of DOM at SG, whereas the specific ultraviolet absorbance (SUVA254) points towards a higher aromaticity of OS DOM (Fig. 8). The incubation did not modified significantly any of the optical properties studied at SG and OS.
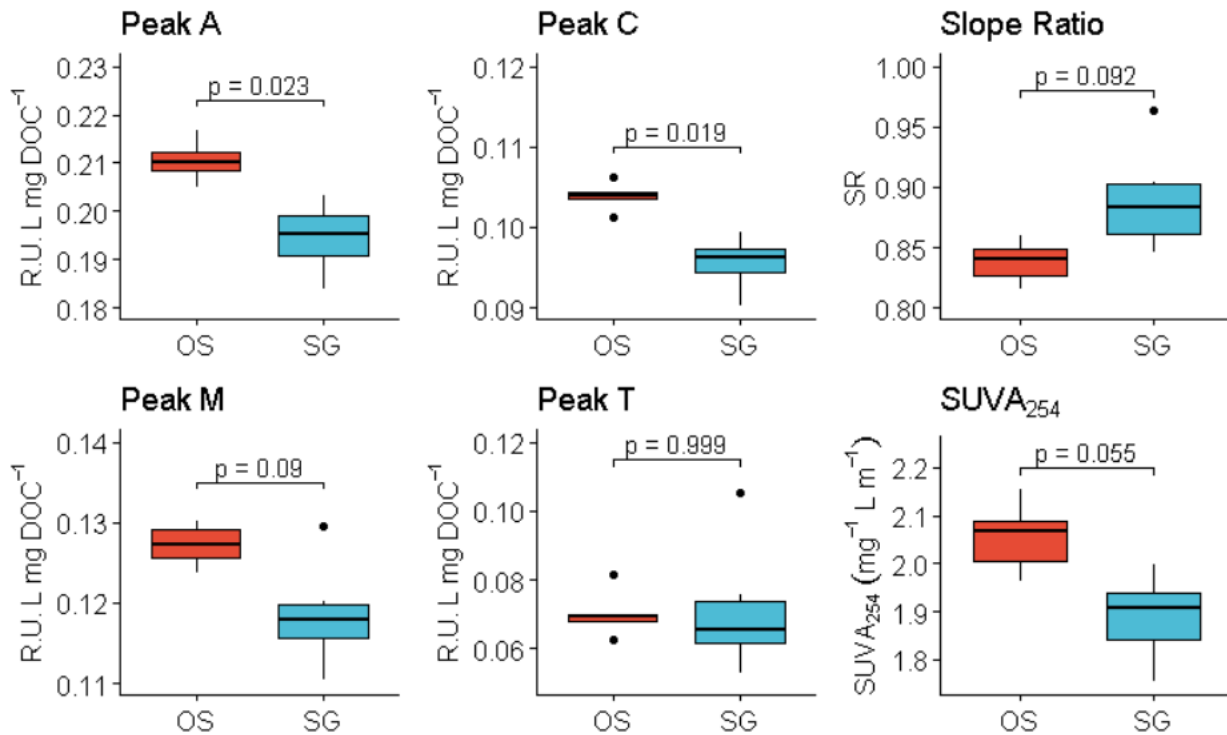
Figure 8. DOC-normalized fluorescence signals of Coble peaks (Peaks A, C, M and T), absorbance slope ratio (SR) and specific ultraviolet absorbance at 254 nm (SUVA254) for Osellino (OS) and San Giuliano (SG) sampling sites.

3.8 Methylation / demethylation rates

Samples spiked with ^{199}Hg and ^{201}Hg to determined methylation and demethylation rates in fresh and incubated cores have been measured in November 2020. Calculations to determine rates are still in progress.

3.9 Analysis of correlation of concentrations in sediments

To better characterize the various relationship between sediment sample and parameters, an analysis of correlation has been performed. Some metallic trace elements (Co, Cu, Zn, Cd, Pb) are well correlated, with r values above 0.9 (Fig. 9). The correlations between these elements extend between sites.
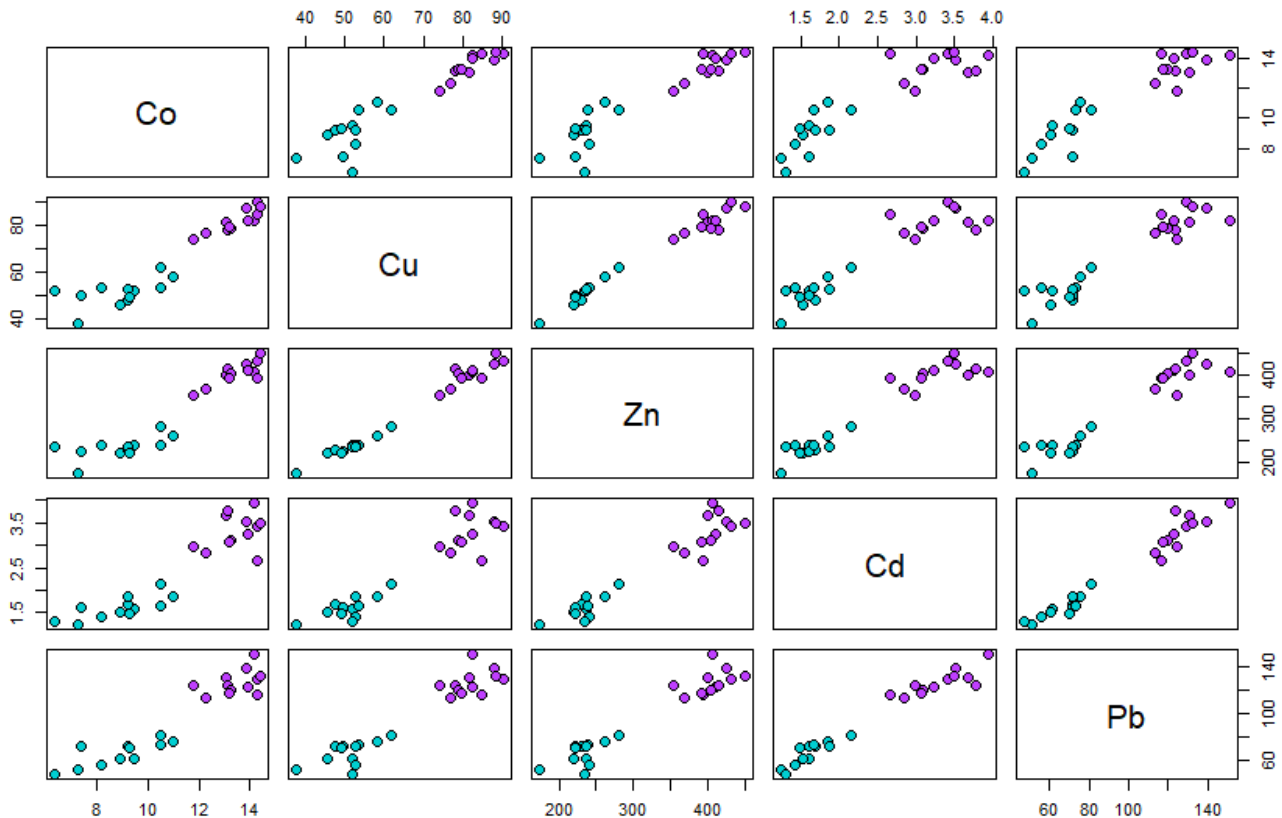
Figure 9. Correlation graphs of selected trace metals, including results from all cores of the two sites (Osellino: purple; San Giuliano: turquoise).

Regarding the correlations between the other measured parameters, some significant correlations are observed within a site (Zn vs. As or Zn vs. Mn in Osellino) but most of the correlation within a site are not significant. Some trends are also observed, with elevated concentrations of two parameters in one site compared to the other (Zn vs. TOC), but no correlation within each site (Fig. 10). This is observed for THg which is higher in SG than in OS, whereas other trace elements show generally a reverse trend.

Total mercury is positively correlated to LOI (r = 0.772 p = 0.003), N (r = 0.736 p = 0.006), and Ptot (r = 0.715 p = 0.009) in OS site, whereas it is only negatively correlated to Cr in SG site (r = 0-0.603 p = 0.038).

MeHg is positively correlated to Ptot in OS (r = 0.711 p = 0.010) and SG (r = 0.772 p = 0.003), and is OS site also to N (r = 0.707 p = 0.004), TOC (r = 0.636 p = 0.026) and THg (r = 0.703 p = 0.011).

It is of note that grain size mean shows no correlation with other parameters, probably as the results of the small range of mean grain size (5.8 to 13.9 µm).

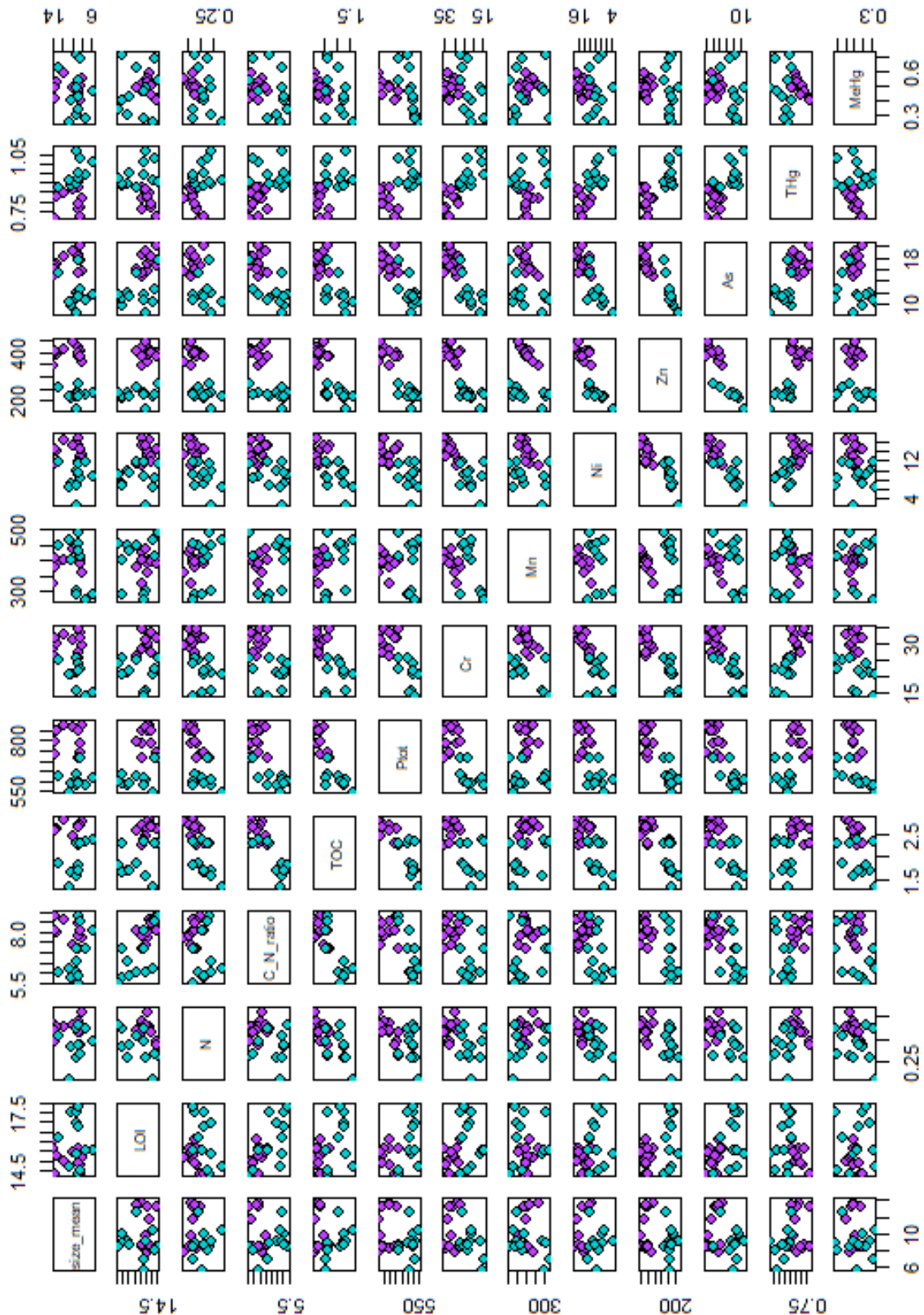Figure 10. Correlation graphs of selected parameters. Zn is used as a surrogate for metals Co, Cu Cd, Pb). (OS purple; SG turquoise).

4. Conclusions on the first field campaign and incubation experiments

From these preliminary interpretations, we observed some differences between the two sites, San Giuliano being slightly more contaminated with Hg than Osellino, with an opposite trend for the other trace elements. On the basis of MeHg concentrations, no signs of increased methylation are recorded, either in overlying water, in surface sediment or in pore water, in the incubated cores compared to the fresh cores in both sites. Hypotheses that explain this lack of evidence are as follow:

i) a real absence of incubation effect of methylation/demethylation rates. The duration of the experiment was too short to achieve anoxia at the sediment water interface and to induce a change in the bacterial activity;

ii) the variations in MeHg concentrations were too small to be detected by the instruments, as the concentrations were often equal to or below the detection limits. However, if this hypothesis is verified, it means that variations were very small, and may not impact seriously the ecosystem;

iii) changes in environmental conditions did altered the methylation and demethylation rates such that the net production remained unchanged. This hypothesis will be verified once the calculations of the methylation/demethylation rates are completed.

Future experiments will be based on these hypotheses, including a possible increase in the experiment duration, performing incubation at a higher temperature to stimulate bacterial activity, improving the analytical resolution to be able to detect smaller changes in MeHg concentrations.

The second field experiment is scheduled for May - June 2021.

References

Behar, F., Beaumont, V., Penteado, H.L.D., 2001. Rock-Eval 6 technology: Performances and developments. Oil & Gas Sci. Technol. 56: 111-134.

Bravo, A.G., Zopfi, J., Buck, M., Xu,J., Bertilsson, S., Schaefer, J.K., Poté, J., Cosio, C., 2018. Geobacteraceae are important members of mercury-methylating microbial communities of sediments impacted by waste water releases. ISME J 12, 802–812.

Chen, H., Zheng, B., Song, Y. Qin, Y., 2011. Correlation between molecular absorption spectral slope ratios and fluorescence humification indices in characterizing CDOM. Aquat Sci. 73: 103–112.

Christensen, G.A., Wymore, A.M., King, A.J., Podar, M., Hurt, R.A. Jr, Santillan, E.U., Soren, A., Brandt, C.C., Brown, S.D., Palumbo, A.V., Wall, J.D., Gilmour, C.C., Elias, D.A., 2016. Development and validation of broad-range qualitative and clade-specific quantitative molecular probes for assessing mercury methylation in the environment. Appl. Environ. Microbiol. 82:6068–6078.

Coble, P.G., 1996. Characterization of marine and terrestrial DOM in seawater using excitation emission matrix spectroscopy. Mar. Chem. 51: 325–346.

Cory, R.M., Mcknight, D.M., Chin, Y.P., Miller, P. Jaros, C.L. 2007. Chemical characteristics of fulvic acids from Arctic surface waters: Microbial contributions and photo-chemical transformations. J. Geophys. Res. Biogeosci.112: G04S51. doi:10.1029/2006JG000343

Espitalié, J., Deroo, G., Marquis, F., 1985a. Rock-Eval Pyrolysis and Its Application 2. Revue de l'IFP 40: 755-784.

Espitalié, J., Deroo, G., Marquis, F., 1985b. Rock-Eval Pyrolysis and Its Applications. Revue de l'IFP 40: 563-579.

Guédron, S., Huguet, L., Vignati, D.A.L., Liu, B., Gimbert, F., Ferrari, B.J.D., Zonta, R., Dominik, J., 2012. Tidal cycling of mercury and methylmercury between sediments and water column in the Venice Lagoon (Italy). Mar. Chem. 130-131: 1-11.

Heiri, O., Lotter, A., Lemcke, G., 2001. Loss on ignition as a method for estimating organic and carbonate content in sediments: reproducibility and comparability of results. J Paleolimnol. 25: 101–110.

Liu, B., Yan, H., Wang, C., Li, Q., Guédron, S., Spangenberg, J.E., Feng, X., Dominik, J., 2012. Insights into low fish mercury bioaccumulation in a mercury-contaminated reservoir, Guizhou, China. Environ. Pollut., 160:109-117.

Loizeau, J.-L., Arbouille, D., Santiago, S., Vernet, J.-P., 1994. Evaluation of a wide range grain size laser diffraction analyser for use with sediments. Sedimentology 41: 353-361.

Fellman, J. B., Hood, E., Spencer, R.G.M., 2010. Fluorescence spectroscopy opens new windows into dissolved organic matter dynamics in freshwater ecosystems: A review. Limnology and Oceanography, 55: 2452–2462.

FOEN (Federal Office for the Environnement), 1998. Ordonnance du 1er juillet 1998 sur les atteintes portées aux sols (Ordinance relating to impacts on the soil). N° RS 814.12. Berne, Switzerland.

Huguet, A., Vacher, L., Relexans, S., Saubusse, S., M.Froidefond, J., Parlanti, E., 2009. Properties of fluorescent dissolved organic matter in the Gironde Estuary. Org. Geochem. 40:706–719.

McKnight, D.M., Boyer, E.W., Westerhoff, P.K., Doran, P.T., Kulbe, T. Andersen, D.T., 2001. Spectrofluorometric characterization of dissolved organic matter for indication of precursor organic material and aromaticity. Limnol.Oceanogr.46: 38–48. doi:10.4319/lo.2001.46.1.0038.

Parlanti, E., Worz, K., Geoffroy, L., Lamotte, M,. 2000. Dissolved organic matter fluorescence spectroscopy as a tool to estimate biological activity in a coastal zone submitted to anthropogenic inputs. Org. Geochem. 31:1765–1781. doi:10.1016/S0146-6380(00)00124-8.

Pucher, M., Wünsch, U., Weigelhofer, G., Murphy, K., Hein, T., Graeber, D., 2019. staRdom: Versatile Software for Analyzing Spectroscopic Data of Dissolved Organic Matter in R. Water 11: 2366.

R Core Team, 2020. R: A language and environment for statistical computing. R Foundation for Statistical Computing, Vienna, Austria. URL https://www.R-project.org/

Rodriguez-Gonzalez, P., Bouchet, S., Monperrus, M., Tessier, E., Amouroux, D., 2013. In situ experiments for element species-specific environmental reactivity of tin and mercury compounds using isotopic tracers and multiple linear regression. Environ. Sci. Pollut. Res. 20: 1269–1280.

US-EPA, 2001. Method 1630, Methyl mercury in water by distillation, Aqueous ethylation, purge and trap, and cold vapor atomic fluorescence spectrometry. EPA 821-R-01-020, 55 pp.

US-EPA, 2002. Method 1631, Revision E: Mercury in water by oxidation, purge and trap, and cold vapor atomic fluorescence spectrometry. EPA-821-R-02-019, 45 pp.

Weishaar, J.L., Aiken, G.R., Bergamaschi, B.A., Fram, M.S., Fujii, R., Mopper K., 2003. Evaluation of specific ultra-violet absorbance as an indicator of the chemical composition and reactivity of dissolved organic carbon. Environ. Sci. Technol. 37: 4702–4708. doi:10.1021/es030360x

Wie, T., Simko, V., 2017. R package "corrplot": Visualization of a Correlation Matrix (Version 0.84). Available from https://github.com/taiyun/corrplot.

Zonta, R., Cassin, D., Pini, R., Dominik, J., 2019. Assessment of heavy metal and As contamination in the surface sediments of Po delta lagoons (Italy). ECSS, 225, doi.org/10.1016/j.ecss.2019.05.017.

Zsolnay, A., Baigar, E., Jimenez, M., Steinweg, B. and Saccomandi, F., 1999. Differentiating with fluorescence spectroscopy the sources of dissolved organic matter in soils subjected to drying. Chemosphere 38: 45–50. doi:10.1016/S0045-6535(98)00166-0

Annex 1: correlation coefficients r and p-values in OS and SG sites

Bold coefficients are statistically significant at level 0.05 (n = 24).

row	column	Osellino site		San Giuliano site	
		r	p	r	p
size_mean	LOI	0.249	0.436	0.166	0.606
size_mean	N	-0.112	0.728	-0.210	0.512
LOI	N	0.546	0.066	0.570	0.053
size_mean	C_N_ratio	0.311	0.325	-0.540	0.070
LOI	C_N_ratio	-0.557	0.060	-0.643	0.024
N	C_N_ratio	-0.382	0.220	-0.087	0.788
size_mean	TOC	0.180	0.576	**-0.601**	**0.039**
LOI	TOC	0.004	0.989	-0.209	0.514
N	TOC	0.556	0.060	0.522	0.082
C_N_ratio	TOC	0.555	0.061	**0.802**	**0.002**
size_mean	Ptot	-0.076	0.815	-0.147	0.647
LOI	Ptot	0.193	0.549	-0.419	0.176
N	Ptot	**0.738**	**0.006**	0.066	0.839
C_N_ratio	Ptot	-0.011	0.973	**0.759**	**0.004**
TOC	Ptot	**0.657**	**0.020**	**0.654**	**0.021**
size_mean	Cr	-0.414	0.181	0.551	0.063
LOI	Cr	-0.248	0.437	0.246	0.440
N	Cr	-0.149	0.644	0.066	0.838
C_N_ratio	Cr	-0.139	0.667	-0.030	0.927
TOC	Cr	-0.258	0.418	-0.027	0.933
Ptot	Cr	-0.269	0.398	0.405	0.191
size_mean	Mn	-0.305	0.335	0.530	0.076
LOI	Mn	-0.191	0.552	-0.077	0.811
N	Mn	-0.247	0.439	-0.416	0.179
C_N_ratio	Mn	-0.048	0.882	-0.155	0.631
TOC	Mn	-0.274	0.388	-0.433	0.160
Ptot	Mn	0.054	0.869	0.124	0.702
Cr	Mn	0.524	0.080	0.652	0.022
size_mean	Ni	-0.305	0.335	-0.039	0.903
LOI	Ni	-0.148	0.647	-0.028	0.932
N	Ni	0.030	0.927	0.386	0.216
C_N_ratio	Ni	-0.234	0.464	0.266	0.403
TOC	Ni	-0.186	0.563	0.440	0.153
Ptot	Ni	0.109	0.737	0.191	0.552
Cr	Ni	**0.808**	**0.001**	0.248	0.436
Mn	Ni	**0.684**	**0.014**	0.298	0.346
size_mean	Zn	-0.106	0.742	0.060	0.853
LOI	Zn	0.056	0.862	-0.212	0.509
N	Zn	-0.068	0.834	0.125	0.698
C_N_ratio	Zn	0.001	0.997	0.456	0.136
TOC	Zn	-0.062	0.848	0.434	0.159
Ptot	Zn	0.293	0.355	0.436	0.157
Cr	Zn	0.313	0.323	0.498	0.100
Mn	Zn	**0.906**	**0.000**	0.513	0.088

row	column	Osellino site		San Giuliano site	
		r	p	r	p
Ni	Zn	0.551	0.064	**0.848**	**0.000**
size_mean	As	-0.392	0.208	0.167	0.604
LOI	As	-0.474	0.120	-0.331	0.293
N	As	-0.303	0.338	0.047	0.886
C_N_ratio	As	0.165	0.608	0.512	0.089
TOC	As	-0.126	0.696	0.427	0.167
Ptot	As	0.257	0.421	**0.666**	**0.018**
Cr	As	0.254	0.426	**0.590**	**0.043**
Mn	As	**0.651**	**0.022**	0.528	0.077
Ni	As	0.446	0.147	**0.702**	**0.011**
Zn	As	**0.638**	**0.026**	0.897	0.000
size_mean	THg	0.167	0.604	-0.517	0.086
LOI	THg	0.772	0.003	-0.440	0.152
N	THg	0.736	0.006	-0.176	0.584
C_N_ratio	THg	-0.305	0.335	0.247	0.440
TOC	THg	0.399	0.199	0.112	0.729
Ptot	THg	0.715	0.009	0.182	0.570
Cr	THg	-0.222	0.489	**-0.603**	**0.038**
Mn	THg	0.040	0.901	-0.431	0.162
Ni	THg	0.089	0.784	-0.504	0.094
Zn	THg	0.382	0.221	-0.546	0.067
As	THg	-0.024	0.942	-0.362	0.247
size_mean	MeHg	0.120	0.711	0.121	0.708
LOI	MeHg	0.412	0.183	-0.090	0.780
N	MeHg	**0.767**	**0.004**	0.228	0.475
C_N_ratio	MeHg	-0.074	0.818	0.423	0.171
TOC	MeHg	**0.636**	**0.026**	0.486	0.109
Ptot	MeHg	**0.711**	**0.010**	**0.772**	**0.003**
Cr	MeHg	0.027	0.933	0.442	0.150
Mn	MeHg	-0.177	0.582	-0.135	0.675
Ni	MeHg	0.187	0.560	-0.084	0.796
Zn	MeHg	0.074	0.818	0.100	0.757
As	MeHg	-0.193	0.548	0.371	0.235
THg	MeHg	**0.703**	**0.011**	0.152	0.637